JOURNAL OF THEORETICAL AND APPLIED MECHANICS
48, 1, pp. 87-109, Warsaw 2010

ACTIVE FENCE WITH FLEXIBLE LINK

Tomasz Piątkowski

University of Technology and Life Sciences, Department of Postal Technology, Bydgoszcz, Poland
e-mail: tomasz.piatkowski@utp.edu.pl

This paper presents the results of research on a model of the sorting process of a unit load stream by means of an active fence with one degree of freedom. In this study, the manipulated loads are treated as bodies of nonlinear elastic-damping properties described by the modified Kelvin model. In investigating the fence structure, one takes into consideration a rigid link and an adjoining flexible link. The equations of motion of the fence flexible link, and those of the interacting object were derived using the finite element method (FEM). The developed model makes it possible to assess the influence of the fence structural and operational parameters on the process of sorting, and evaluate dynamic forces exerted on the manipulated loads.

Key words: unit load, handling process, belt conveyor, sorting, active fence

1. Introduction

One of technical solutions utilised in logistic centres for automated distribution of streams of small-size unit loads (i.e. mail parcels) into diverse directions of transportation is the application of scrapping devices in the transport system. These devices are allocated along the transporting conveyor, and their executing elements are e.g. fences, which perform pendulous motion (Piątkowski and Sempruch, 2002 – Fig. 1a). Such a solution (due to its uncomplicated structure) is characterised by good functionality, high strength and reliability of operation, which significantly increases the overall effectiveness of the sorting system. In these solutions, the fence together with its driving system usually constitutes a structure of very high rigidity. Such a property guarantees the realisation of the assumed trajectory of the fence motion, irrespective of the loading forces. However, such a concept does not satisfy the requirements of

contemporary logistic processes in which one aims at achieving higher and higher speeds of the object transportation at the same time minimizing dynamic interactions generated while performing manipulation actions on the objects. The consequence of applying sorting devices of highly rigid structure is the lack of possibility to absorb and dissipate the impact energy released when the load enters into contact with the fence. In such a case, the conditions of obtaining high effectiveness of the sorting process, and preventing the load from mechanical damage, are difficult to be brought together.

It is known from the world literature that the mechanical system consisting of a belt conveyor and an arm (active rotary fence, or a number of passive fences) placed above the belt finds its application in mechanisation of the positioning process. This process consists in giving the loads a precisely defined destination position (rotary and translational – Mason, 1999). In the studies pertaining to this application of fences (Akella *et al.*, 2000; Akella and Mason, 1998; Berretty *et al.*, 1998; Mason, 1986; Stappen and Gldberg, 2000), the problem of interaction between the fence and the load is reduced to quasi-statistic events only – the inertia forces are neglected. It is assumed in these works that the process of positioning is carried out at a low transportation speed of the conveyor, owing to which the dynamic reaction forces are negligibly small in comparison with the friction forces.

The problem of mitigating reaction forces in the sorting process was considered in the work by Piątkowski and Sempruch (2005), where the authors discussed a solution consisting in replacing the classic straight-linear fence with a curvilinear one, modelled upon the Bézier curve. In work by Piątkowski (2004), one analyses the application of a pneumatic system in the fence drive, and in Piątkowski and Sempruch (2006) one proposes a rocker mechanism and a worm gear joined by a flexible clutch. These examples do not exhaust all possible constructional solutions aimed at decreasing the dynamic reaction forces exerted on the manipulated loads. Softening of impact effects in the sorting process can also be achieved by utilising a fence of adequately chosen constructional rigidity, i.e. the flexible fence presented in Piątkowski and Sempruch (2008). The considered fence was treated there as a beam made entirely of a homogeneous material. For constructional reasons, making and utilising such a fence is troublesome. A more rational solution would be the fence (Fig. 1b) which consists of two elements: a rigid one (used for joining the fence with the frame and the drive system of the sorting device), and a flexible element of constant bending strength (responsible for softening the effects of impact on the object). The theoretical analysis of application of such a fence is presented in this paper.

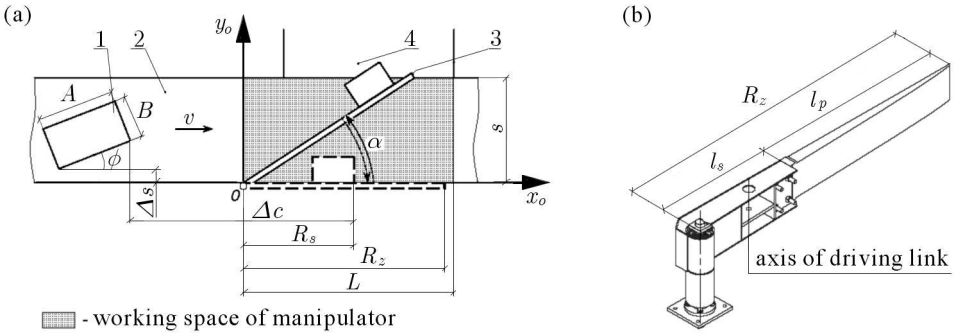

Fig. 1. Example of manipulator with rotary active fence: (a) scheme of sorting assembly, (b) fence with flexible element; 1 – unit load, 2 – main conveyor, 3 – active fence, 4 – chute; s – width of conveyor, Δs – distance between load and conveyor border, R_s – position of load front at starting moment of fence operation, R_z – length of fence, Δc – distance between loads fronts, L – length of manipulator working space, $A \times B$ – dimensions of load, ϕ – load position angle, α – fence deflection angle, v – conveyor transportation speed, l_s, l_p – lengths of rigid and flexible links of fence, respectively

2. Model of load motion

2.1. Assumptions for developing physical model

In the physical model of the sorting process, which is treated as the first stage in formulation of a computer model, one takes the following assumptions:

- the sorting process is assumed to be a planar motion on the plane of main conveyor,
- the load has a rectangular shape (in the projection on the main conveyor plane),
- friction forces are modelled according to Coulomb's law (Kikuuwe *et al.*, 2005),
- the resulting friction forces and moments of friction in the planar motion are described according to the model proposed in the work by Goyal *et al.* (1991),
- the rigid link of the fence is fixed at one end, and is set in rotary motion α_w by the drive system (Fig. 2a),
- the flexible link is treated as a continuous system (Jalili and Esmailzadeh, 2002; Wittbrodt *et al.*, 2006) discretised according to the finite element method (FEM) (Gawroński *et al.*, 1984; Zienkiewicz, 2000) implemented in the Matlab environment,

- the transversal cross-section of the flexible link of the fence has constant bending strength, which is achieved by giving it a variable thickness according to the formula

$$h = h_1 \sqrt{\frac{l_p - x}{l_p}} \tag{2.1}$$

where

h_1 – initial thickness of the fence flexible link
l_p – length of the fence flexible link
x – coordinate of the flexible link cross-section position ($x = 0$ – point joining rigid link with the flexible one).

- two-node beam elements are applied in the discrete model of the fence (Fig. 2b), in which every node is subject to translational q_3, and rotational displacement q_5,
- the reaction force appearing between the object and the fence is described based on a modified nonlinear Kelvin's model (Piątkowski and Sempruch, 2009)

$$N = b_p m_p^{0.4} \dot{D} D^2 + k_p D^4 \tag{2.2}$$

where

$D, \dot{D}$ – strain [m] and strain velocity [m/s] of colliding bodies
b_p, k_p – damping [Nskg$^{-0.4}$m^{-3}] and stiffness [Nm^{-4}] factors
m_p – mass of the load [kg].

The values of exponents of power functions in the formulae that describe local deformation of the bodies (in Eq. (2.2)) were chosen based on the results of numerical experiments. These were aimed at finding a good mathematical representation for the actual impact course registered in experimental investigations. The factor $m_p^{0.4}$ introduced into the model allows us to obtain a constant value of the restitution coefficient (for the assumed parameters b_p and k_p), irrespective of the masses of bodies used in impact simulation. Effectiveness of the model (Eq. (2.2)) in predicting the course of impact was confirmed by experimental investigations carried out in dynamic load conditions: when the object impacts into a deformable and undeformable obstacle (Piątkowski and Sempruch, 2009).

In order to simplify the dynamic analysis, the continuous process of sorting was subjected to discretisation – division of the process into individual stages. The kinematic-dynamic characteristics of the load, which result from mutual interaction between the load and the fence, differ significantly in each stage.

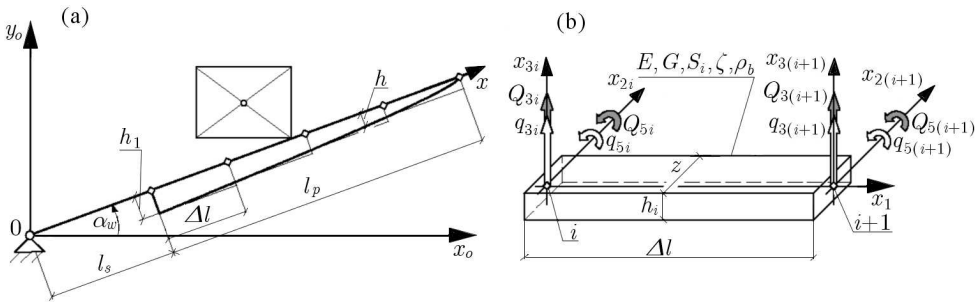

Fig. 2. Division of fence flexible link into discrete FEMs: (a) discrete model of fence, (b) two-node discrete beam model; q_3, q_5 – generalised coordinates (two degrees of freedom: translation and rotation), Q_3, Q_5 – generalized forces, E – Young's modulus, G – shear (Kirchhoff's) modulus, $S_i = zh_i$ – area of transverse cross-section, ζ – material damping (Giergiel, 1990), ρ_b – mass density, α_w – angular position of fence driving link, Δl – length of discrete element, l_s, l_p – length of fence rigid and flexible link, respectively

Each characteristic stage of load motion needs an individual mathematical description, and this has form of a separate module of the numerical model code. Simulation of the model consists in running the modules in a sequence, according to the position currently taken by the load with respect to the executing elements of the manipulator.

Taking into account author's previous experience in numerical simulation of the sorting process models (Piątkowski and Sempruch, 2002, 2008), it was assumed that the following characteristic stages must be taken into account in order to recognise the basic characteristics of load distribution process realised by means of an active fence with a flexible link:

- oblique impact of the load against the fence,
- motion of the load along the fence,
- motion of the load along the conveyor border: one of load corners slides along the border of the conveyor, the other one along the fence,
- free motion of the load.

In the last of the mentioned stages, physical properties of the fence have no influence on behaviour of the load (no contact with the fence). For this reason, we do not present here any mathematical description of the load free motion, assuming that it does not differ from that presented in the work by Piątkowski and Sempruch (2002).

Four reference coordinate systems were assumed in the determination of the equations of the physical model (Fig. 3 – Fig. 7):

- rectangular Ox_oy_o, connected with the manipulator frame, whose origin lies on the fence rotation axis – this one was applied in presentation of the results of load motion simulation,
- rectangular Oy_pz_p, connected with the load – applied for determination of the position of the load gravity centre with respect to its geometric centre,
- rectangular Ox_3x_1, connected with a specific discrete element – applied in description of physical properties of discrete elements of the fence,
- polar coordinate system, with radius-vector $\boldsymbol{r}$ and polar angle α_p – applied in deriving the equations of load motion.

2.2. Oblique impact of load against fence

This kind of impact of the load against the fence (Fig. 3) takes place when the load (just before entering in contact with the fence) is positioned arbitrarily within the available width of the conveyor.

The system of equations of forces and moments acting on the load and the fence in this stage of the sorting process can be presented as (see Fig. 3)

$$\begin{aligned}
&\mathbf{M}_b\ddot{\boldsymbol{q}} + \mathbf{B}_b\dot{\boldsymbol{q}} + \mathbf{K}_b\boldsymbol{q} = \boldsymbol{Q}\\
&m_p\ddot{r} = F_\xi + P_{cen} - F_2\cos(\alpha_p - q_{5(N)}) + N\sin(\alpha_p - q_{5(N)})\\
&m_p r\ddot{\alpha}_p = -F_\eta - P_{Cor} + F_2\sin(\alpha_p - q_{5(N)}) + N\cos(\alpha_p - q_{5(N)})\\
&I_p\ddot{\phi} = -r_{Cj}\left[u_jN\cos\left(\gamma_j + u_j(\phi - q_{5(N)})\right) + F_2\sin\left(\gamma_j + u_j(\phi - q_{5(N)})\right)\right] - T
\end{aligned} \tag{2.3}$$

where

j – number of the load corner being in contact with the fence, $j = 1, 2, 3, 4$

i – number of node of the fence discrete element being in contact with the load, $i = 1, 2, 3, \ldots, n_E + 1$

n – number of degrees of freedom of nodes in the fence discrete model, $n = 2(n_E + 1)$

n_E – number of discrete elements

$\mathbf{M}_b, \mathbf{B}_b, \mathbf{K}_b$ – matrices of inertia, damping and rigidity of the fence discrete model, of dimensions $n \times n$

$\boldsymbol{q}$ – vector of generalised displacements of nodes, of dimensions $n \times 1$

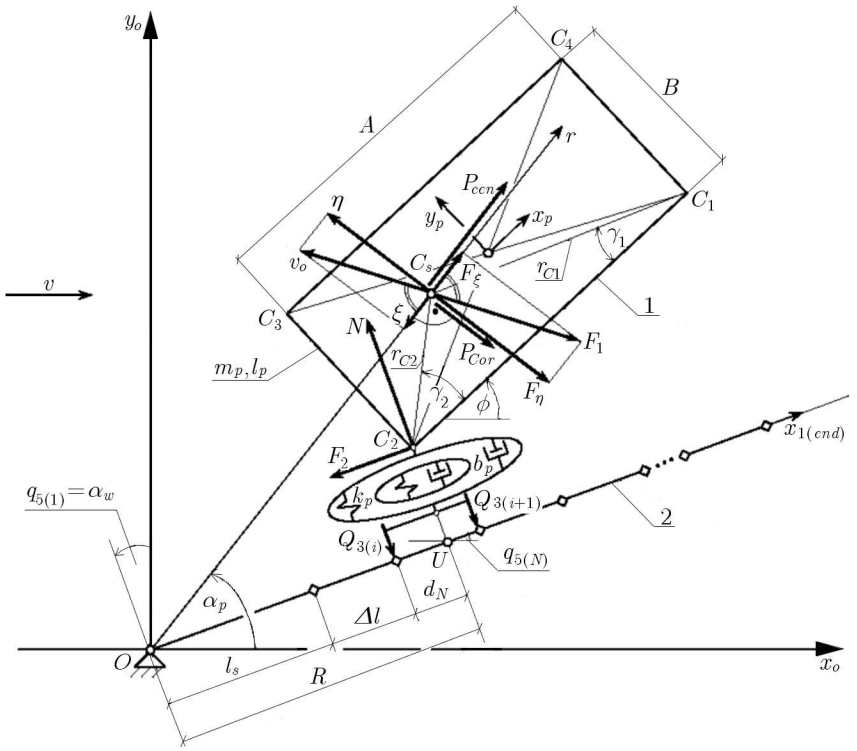

Fig. 3. Scheme of forces acting on load during its impact against active fence; 1 – load, 2 – fence

$\boldsymbol{Q}$ – vector of generalised forces acting on nodes of discrete elements, of dimensions $n \times 1$

$q_{5(N)}$ – angular position of the fence discrete element at its contact point with the load U – according to Eq. (2.22)

$Q_{3(i)}$ – external force exerted on the i-th node of the discrete element

$q_{5(1)} = \alpha_w$ – angular position of the first node of the discrete element

m_p, I_p – load mass and mass moment of inertia

ϕ – rotation angle of load

N – force of reaction between the load and fence in the normal direction of impact – according to Eq. (2.2)

P_{Cor}, P_{cen} – Coriolis force and centrifugal force

$$P_{Cor} = 2m_p\dot{\alpha}_p\dot{r} \qquad P_{cen} = m_p\dot{\alpha}_p^2 r \tag{2.4}$$

The first equation in (2.3) is a matrix equation of motion of discrete elements of the fence. The remaining equations describe motion of the load in the polar coordinate system with the radius-vector r and polar angle α_p.

Depending on which of the load corners C_j is in contact with the fence, the length of the radius-vector r_{Cj} connecting the corner C_j $(j = 1, 2, 3, 4)$ with gravity centre of the load C_s is equal to

$$r_{Cj} = \begin{cases} \sqrt{(0.5A + (3-j)x_p)^2 + (0.5B + (3-j)y_p)^2} & \text{if} \quad j = 2, 4 \\ \sqrt{(0.5A - (2-j)x_p)^2 + (0.5B + (2-j)y_p)^2} & \text{otherwise} \end{cases} \tag{2.5}$$

The position angle of the load gravity centre γ_j is defined by the relationship

$$\gamma_j = \begin{cases} \arcsin \dfrac{0.5B + y_p}{r_{Cj}} & \text{if} \quad j = 1, 2 \\ \arcsin \dfrac{0.5B - y_p}{r_{Cj}} & \text{otherwise} \end{cases} \tag{2.6}$$

and the factor u_j appearing in (2.3) is defined as

$$u_j = \begin{cases} 1 & \text{if} \quad j = 2, 4 \\ -1 & \text{otherwise} \end{cases} \tag{2.7}$$

For the reaction force N between the object and the load be continuously and uniformly transmitted, one assumes that adjacent nodes of discrete elements are simultaneously subjected to adequately reduced generalised forces $Q_{3(i)}$ and $Q_{3(i+1)}$, according to the following proportions

$$Q_{3(i)} = N\Big(1 - \frac{d_N}{\Delta l}\Big) \qquad Q_{3(i+1)} = N\frac{d_N}{\Delta l} \tag{2.8}$$

where

Δl – length of the discrete element, $\Delta l = l_p/n_E$

l_p – length of the fence flexible link.

The reduction is carried out taking into account the principle of equilibrium of action and reaction forces and moments, according to geometric relationships shown in Fig. 4.

Assuming that the deflection angle of fence (under the pressure of object – Fig. 3, Fig. 4), is small, the number of the fence discrete element being in contact with the object can be determined as the integer portion of the qu-

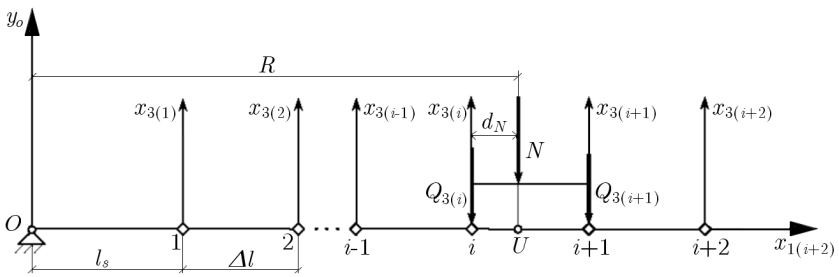

Fig. 4. Forces exerted by object on fence

otient of $R - l_p$ and Δl (assuming $R > l_p$, and applying the Matlab function "floor")

$$i = \begin{cases} \text{floor}\Big(\dfrac{R - l_p}{\Delta l}\Big) + 1 & \text{if} \quad \text{floor}\Big(\frac{R-l_p}{\Delta l}\Big) + 1 < n_E \\ \text{error} & \text{otherwise} \end{cases} \tag{2.9}$$

and the segment dN is the reminder of this quotient

$$d_N = \text{mod}\Big(\frac{R - l_s}{\Delta l}\Big) \tag{2.10}$$

The distance between the corner C_j and rotation axis of the fence is given by the formula

$$R = \sqrt{x_{oC}^2 + y_{oC}^2} \tag{2.11}$$

where the coordinates x_{oC}, y_{oC} of the point C_j can be expressed as

$$\begin{aligned} x_{oC} &= r\cos\alpha_p - u_j r_{Cj}\cos(\gamma_j + \phi) \\ y_{oC} &= r\sin\alpha_p - r_{Cj}\sin(\gamma_j + \phi) \end{aligned} \tag{2.12}$$

Deformation of the load at the contact point C_j in the normal impact direction (necessary for determination of the reaction force N) is the shortest distance between the fence and the load corner. This distance is defined by the length of segment connecting the points C_j and U (see Fig. 3)

$$D = \frac{y_{oU} - y_{oC}}{\cos q_{5(N)}} \tag{2.13}$$

The point U lying on the surface of the fence is determined based on the assumption that, as the fence deflects making its rotary motion, the distance

Δl between adjacent nodes of discrete elements remains constant, and translational dislocations of the nodes q_3 are represented by the arches drawn by the ends of discrete elements – as shown in Fig. 5. The coordinates of point U are

$$\begin{aligned} x_{oU} &= l_s \cos\alpha_w + d_N \cos\vartheta_N + \sum_{k=1}^{i-1} \Delta l \cos\vartheta_k \\ y_{oU} &= l_s \sin\alpha_w + d_N \sin\vartheta_N + \sum_{k=1}^{i-1} \Delta l \sin\vartheta_k \end{aligned} \tag{2.14}$$

where

ϑ_k – angle between the straight line passing through nodes k and $k+1$ and the abscissa axis of Ox_oy_o system (Fig. 5)

$$\vartheta_k = \frac{q_{3(k+1)} - q_{3(k)}}{\Delta l} \tag{2.15}$$

ϑ_N – angle between the straight line passing through the points U and node i and the abscissa axis of Ox_oy_o system

$$\vartheta_N = \frac{q_{3(N)} - q_{3(i)}}{d_N} \tag{2.16}$$

$q_{3(N)}, q_{5(N)}$ – coordinates of the point U in the rectangular coordinate system Ox_3x_1, calculated on the basis of the polynomial approximation of dislocation within discrete elements (Gawroński *et al.*, 1984)

$$\begin{aligned} q_{3(N)} &= q_3(d_N) = p_1 + p_2 d_N + p_3 d_N^2 + p_4 d_N^3 \\ q_{5(N)} &= q_5(d_N) = p_2 + 2p_3 d_N + 3p_4 d_N^2 \end{aligned} \tag{2.17}$$

$\boldsymbol{p} = [p_1, p_2, p_3, p_4]$ – vector of coefficients determined on the basis of boundary conditions $q_3(0)$, $q_5(0)$, $q_3(\Delta l)$ and $q_5(\Delta l)$ substituted into Eqs. (2.17).

The speed of load deformation during the impact can be written as

$$\dot{D} = \frac{d}{dt}(D) \tag{2.18}$$

The manipulated object can dislocate with respect to both the carrying surface of the conveyor, and the fence; it can also remain immobile with respect to one of these surfaces. However, the situation when the load is immobile with

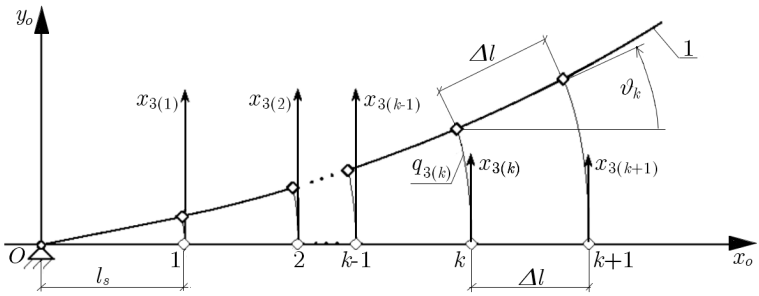

Fig. 5. Interpretation of translational displacements of discrete element nodes of fence moving in rotational motion; 1 – fence, $q_{3(k)}$ – translational displacement of node k

respect to both surfaces should not take place. The variants of motion, in which the object slides with respect to the working surfaces, are taken into account hereunder in descriptions. The kind of load friction, static or kinematic one, was identified in each of these variants.

The components F_ξ and F_η of the friction force F_1 for the load sliding on the conveyor carrying surface, the friction moment T appearing in planar motion of the load, and the friction force F_2 of the load with respect to the fence, are determined by the following relationships

$$F_\xi = \begin{cases} \dfrac{\xi F_{max}}{v_o\sqrt{1+\left(\frac{T_{max}\dot{\phi}}{F_{max}v_o}\right)^2}} & \text{if} \quad v_o > 0 \\ \left\{\begin{array}{ll} P_{\xi ext} & \text{if} \quad F_{max} > P_{1ext} \\ F_{max}\dfrac{P_{\xi ext}}{P_{1ext}} & \text{otherwise} \end{array}\right\} & \text{otherwise} \end{cases}$$

$$F_\eta = \begin{cases} \dfrac{\eta F_{max}}{v_o\sqrt{1+\left(\frac{T_{max}\dot{\phi}}{F_{max}v_o}\right)^2}} & \text{if} \quad v_o > 0 \\ \left\{\begin{array}{ll} P_{\eta ext} & \text{if} \quad F_{max} > P_{1ext} \\ F_{max}\dfrac{P_{\eta ext}}{P_{1ext}} & \text{otherwise} \end{array}\right\} & \text{otherwise} \end{cases} \tag{2.19}$$

$$T = \begin{cases} \dfrac{T_{max}\,\mathrm{sgn}\,(\dot{\phi})}{\sqrt{1+\left(\frac{F_{max}v_o}{T_{max}\dot{\phi}}\right)^2}} & \text{if} \quad |\dot{\phi}| > 0 \\ \left\{\begin{array}{ll} T_{ext} & \text{if} \quad T_{max} > |T_{ext}| \\ T_{max}\,\mathrm{sgn}\,(T_{ext}) & \text{otherwise} \end{array}\right\} & \text{otherwise} \end{cases}$$

$$F_2 = \begin{cases} N\mu_2 \operatorname{sgn}(w_{xj}) & \text{if} \quad |w_{xj}| > 0 \\ \left\{ \begin{array}{ll} P_{2ext} & \text{if} \quad N\mu_2 > |P_{2ext}| \\ N\mu_2 \operatorname{sgn}(P_{2ext}) & \text{otherwise} \end{array} \right\} & \text{otherwise} \end{cases}$$

where

F_{max}, T_{max} – maximum friction force and maximum friction moment appearing in the case of pure translational or pure rotational motion of the load

$$F_{max} = m_p g \mu_1 \qquad T_{max} = \frac{m_p g}{S} \mu_1 \int_S r_S \, dS \tag{2.20}$$

g – acceleration of gravity

μ_1, μ_2 – friction coefficients of the load with respect to carrying surfaces of the conveyor and fence, respectively

S – area of contact between the load and friction surface

dS – infinitesimal friction surface

r_S – distance between an infinitesimal friction surface dS and the gravity centre of load

P_{1ext} – resultant external force exerted by the fence on the object

$$P_{1ext} = \sqrt{P_{\xi ext}^2 + P_{\eta ext}^2} \tag{2.21}$$

$P_{\xi ext}, P_{\eta ext}$ – components of the force P_{1ext}

$$\begin{aligned} P_{\xi ext} &= N[\mu_2 \operatorname{sgn}(w_{xj}) \cos(\alpha_p - q_{5(N)}) - \sin(\alpha_p - q_{5(N)})] \\ P_{\eta ext} &= N[(\mu_2 \operatorname{sgn}(w_{xj}) \sin(\alpha_p - q_{5(N)}) + \cos(\alpha_p - q_{5(N)})] \end{aligned} \tag{2.22}$$

T_{ext} – moment of external forces exerted on the object

$$T_{ext} = -r_{Cj} N[u_j \cos(\gamma_j + u_j(\phi - q_{5(N)})) + \mu_2 \operatorname{sgn}(w_{xj}) \sin(\gamma_j + u_j(\phi - q_{5(N)}))] \tag{2.23}$$

P_{2ext} – external force, tangent to the fence, exerted by frictional coupling existing between the object and carrying surface of the conveyor

$$P_{2ext} = F_\xi \cos(\alpha_p - q_{5(N)}) + F_\eta \sin(\alpha_p - q_{5(N)}) \tag{2.24}$$

w_{xj} – speed of sliding of the load corner with respect to the fence

$$\begin{aligned} w_{xj} = \dot{r} \cos(\alpha_p - q_{5(N)}) - r(\dot{\alpha}_p - \dot{q}_{5(N)}) \sin(\alpha_p - q_{5(N)}) + \\ + r_{Cj}(\dot{\phi} - \dot{q}_{5(N)}) \sin(\gamma_j + u_j(\phi - q_{5(N)})) \end{aligned} \tag{2.25}$$

The values of components ξ and η of the vector of relative friction speed v_o of the load gravity centre C_s on the conveyor belt are equal to

$$\xi = v\cos\alpha_p - \dot{r} \qquad \eta = v\sin\alpha_p + r\dot{\alpha}_p \tag{2.26}$$

2.3. Motion of load along fence

The stage of motion in which the load slides along the fence (Fig. 6) takes place when the load is transported near the conveyor border on that side, where the fence is mounted. This stage can also be a continuation of load motion after its oblique impact against the fence – after which the load rotates and takes the position parallel to the fence.

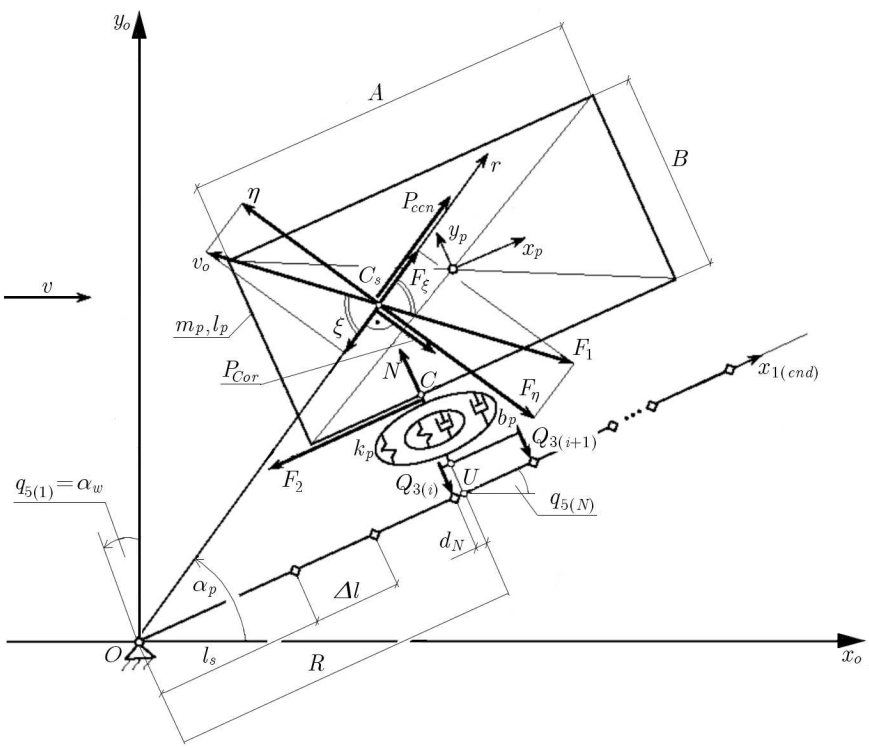

Fig. 6. Scheme of forces acting on load moving along fence

Dynamic interactions between the load and the fence can be expressed by equations (according to Fig. 6)

$$\begin{aligned}
&\mathbf{M}_b\ddot{\boldsymbol{q}} + \mathbf{B}_b\dot{\boldsymbol{q}} + \mathbf{K}_b\boldsymbol{q} = \boldsymbol{Q}\\
&m_p\ddot{r} = F_\xi - F_2\cos(\alpha_p - q_{5(N)}) + N\sin(\alpha_p - q_{5(N)}) + P_{cen}\\
&(m_p r^2 + I_p)\ddot{\alpha}_p = [F_2\sin(\alpha_p - q_{5(N)}) + N\cos(\alpha_p - q_{5(N)}) - F_\eta - P_{Cor}]r - T
\end{aligned} \tag{2.27}$$

Denotations of quantities used in these equations are the same as those in Eqs. (2.3).

The reaction forces between the object and the fence are applied at the point C, which is a rectangular projection of the object centre of gravity C_s on the wall of load that touches the fence.

The components of external force $P_{\xi ext}$, $P_{\eta ext}$ exerted on the object (which are required for determination of the force of friction between the object and the conveyor, according to $(2.19)_{1,2,3}$ take the form

$$\begin{aligned}
P_{\xi ext} &= N[\mu_2\,\mathrm{sgn}\,(w_x)\cos(\alpha_p - q_{5(N)}) - \sin(\alpha_p - q_{5(N)})]\\
P_{\eta ext} &= N[\mu_2\,\mathrm{sgn}\,(w_x)\sin(\alpha_p - q_{5(N)}) + \cos(\alpha_p - q_{5(N)})] - \frac{T}{r}
\end{aligned} \tag{2.28}$$

The sliding speed of the object with respect to the fence, which appears in $(2.19)_4$, is

$$w_x = \dot{r}\cos(\alpha_p - q_{5(N)}) - r(\dot{\alpha}_p - \dot{q}_{5(N)})\sin(\alpha_p - q_{5(N)}) \tag{2.29}$$

The coordinates of the point C, necessary for determination of the distance R from the i-th node of the fence discrete element being in contact with the object, are equal to (according to Fig. 6)

$$\begin{aligned}
x_{oC} &= r\cos\alpha_p + \frac{1}{2}(B + y_p)\sin q_{5(N)}\\
y_{oC} &= r\sin\alpha_p - \frac{1}{2}(B + y_p)\cos q_{5(N)}
\end{aligned} \tag{2.30}$$

2.4. Motion of load with one corner sliding along border of conveyor, and another one along fence

In the case when the load transported by the conveyor lies just next to its border (at the side where the fence is mounted), there could exist a situation when one of the load corners slides along the border of the conveyor, and another one along the fence (Fig. 7). Then, the load is lead out from the stream of loads in the result of impact-free sliding along the fence.

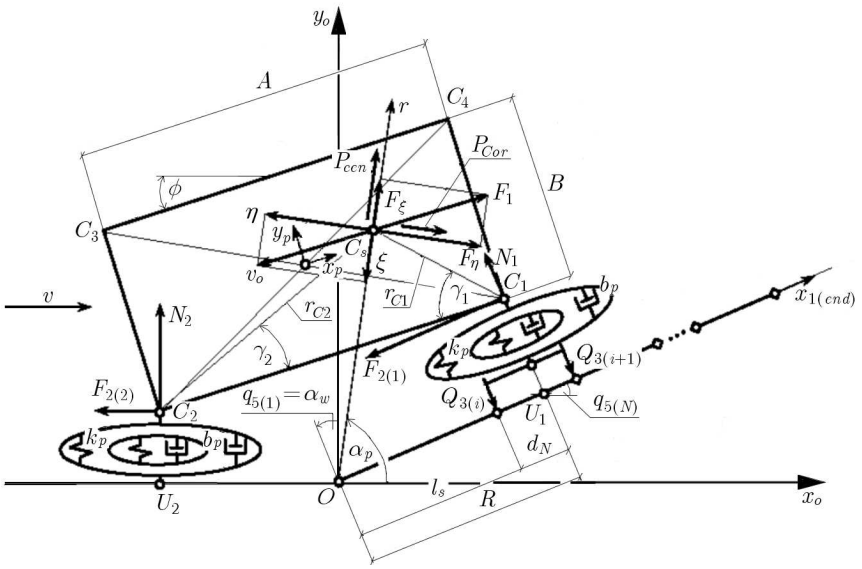

Fig. 7. Scheme of forces acting on load whose one corner rubs against border of conveyor, and another one against fence

The load and fence motions can be described by the following equations – according to Fig. 7:

$$\mathbf{M}_b\ddot{\boldsymbol{q}} + \mathbf{B}_b\dot{\boldsymbol{q}} + \mathbf{K}_b\boldsymbol{q} = \boldsymbol{Q}$$

$$\begin{aligned}
m_p\ddot{r} &= F_\xi + P_{cen} + N_2\sin\alpha_p - F_{2(2)}\cos\alpha_p + N_1\sin(\alpha_p - q_{5(N)}) + \\
&\quad -F_{2(1)}\cos(\alpha_p - q_{5(N)}) \\
m_p r\ddot{\alpha}_p &= -F_\eta - P_{Cor} + N_2\cos\alpha_p + F_{2(2)}\sin\alpha_p + N_1\cos(\alpha_p - q_{5(N)}) + \\
&\quad +F_{2(1)}\sin(\alpha_p - q_{5(N)}) \\
I_p\ddot{\phi} &= r_{C1}[N_1\cos(q_{5(N)} + \gamma_1 - \phi) - F_{2(1)}\sin(q_{5(N)} + \gamma_1 - \phi)] + \\
&\quad -r_{C2}[N_2\cos(\gamma_2 + \phi) + F_{2(2)}\sin(\gamma_2 + \phi)] - T
\end{aligned} \tag{2.31}$$

In the case of static friction between the load and the conveyor, the reaction forces and the moments exerted on the object (required in $(2.19)_{1,2,3}$) take the form

$$\begin{aligned}
P_{\xi ext} &= -N_2\sin\alpha_p + F_{2(2)}\cos\alpha_p - N_1\sin(\alpha_p - q_{5(N)}) + F_{2(1)}\cos(\alpha_p - q_{5(N)}) \\
P_{\eta ext} &= N_2\cos\alpha_p + F_{2(2)}\sin\alpha_p + N_1\cos(\alpha_p - q_{5(N)}) + F_{2(1)}\sin(\alpha_p - q_{5(N)}) \\
T_{ext} &= r_{C1}[N_1\cos(q_{5(N)} + \gamma_1 - \phi) - F_{2(1)}\sin(q_{5(N)} + \gamma_1 - \phi)] + \\
&\quad -r_{C2}[N_2\cos(\gamma_2 + \phi) + F_{2(2)}\sin(\gamma_2 + \phi)]
\end{aligned} \tag{2.32}$$

The sliding speeds of the object corners, w_{x1} – referred to the fence at the contact point C_1 and w_{x2} – referred to the conveyor border at the point C_2, are given by equations

$$\begin{aligned} w_{x1} &= \dot{r}\cos(\alpha_p - q_{5(N)}) - r(\dot{\alpha}_p - \dot{q}_{5(N)})\sin(\alpha_p - q_{5(N)}) + \\ &\quad + r_{C1}(\dot{\alpha}_p - \dot{q}_{5(N)})\sin(\alpha + \gamma_1 - \phi) \\ w_{x2} &= \dot{r}\cos\alpha_p - r\dot{\alpha}_p \sin\alpha_p + r_{C2}\dot{\phi}\sin(\gamma_2 + \phi) \end{aligned} \tag{2.33}$$

Due to conditions existing during sorting, these speeds take values greater than zero – which was confirmed in preliminary investigations. For this reason, we assume that only kinetic friction exists at the points C_j $(j = 1, 2)$, and $F_{2(j)} = N_{(j)}\mu_2$ – according to Eq. $(2.19)_4$.

Deformation of the object at the contact point C_2 is

$$D = -y_{oC2} \tag{2.34}$$

where y_{oC2} – ordinate of the point C_2 in the coordinate system Ox_oy_o.

The remaining denotations are the same as those in description of Eqs. (2.3).

3. Numerical investigations

In the simulation investigations carried out in this study, we considered two variants of the fence: the first variant pertaining to the fence composed of two links (a rigid one and a flexible one, of dimensions $l_s = 0.45\,\mathrm{m}$, $l_p = 0.75\,\mathrm{m}$, $z \times h_1 = 0.132 \times 0.045\,\mathrm{m}$), and the second variant – the fence made entirely of a homogeneous material ($l_s = 0\,\mathrm{m}$, $l_p = 1.2\,\mathrm{m}$, $z \times h_1 = 0.132 \times 0.073\,\mathrm{m}$). It was assumed that the flexible links are made of polyamide PA6 – a material characterised by high internal damping and high mechanical strength (Basf technical resources (2008)). The proportion of the rigid link length to the length of the flexible one (in the first variant of the fence structure) was assumed taking into account the need for ensuring enough space necessary to easily couple the rigid link to the frame and to the drive system of the sorting device.

The maximum relative impact speed in the normal object-fence direction is equivalent to the speed which the object reaches during free fall from the height of $H = 0.3\,\mathrm{m}$ on an undeformable ground – that is the fall treated in this work as the admissible hazard due to dynamic reactions exerted on the object. The mechanical properties of the sorted load ($b_p = 3.3 \cdot 10^5\,\mathrm{Nskg^{-0.4}m^{-3}}$;

$k_p = 1.72 \cdot 10^9\,\mathrm{Nm}^{-4}$), required in Eq. (2.2), were assumed on the basis of experimental and numerical investigations of impacts of unit loads described in work by Piątkowski and Sempruch (2009). The linear speed of load transportation on the main conveyor and the rotational speed of the fence are selected so that reliable sorting of loads and the maximum sorting capacity of the system can be achieved (Piątkowski and Sempruch, 2002).

3.1. Simulation of impact of object against fence

The courses of dynamic processes that take place when the object impacts against the fence are presented in Fig. 8-Fig. 10. The point marked 1 in the graphs (Fig. 8) pertains to the moment of impact initiation, while point 2 denotes the end of impact.

The impact process was arranged in a special way so as to evoke maximal dynamic reactions. Before the impact, the load was positioned and oriented on the conveyor in such a position that during impact initiation the load collided into the part of the fence most distant from the rotation axis, and the gravity centre of load C_s was on the normal of impact.

The transverse dimensions of flexible links of the examined fences were chosen in such a way that, even with the most difficult impact conditions predicted for this experiment (as described above, for the parameters: main conveyor transportation speed $v = 2\,\mathrm{m/s}$, load mass $m_p = 15\,\mathrm{kg}$, the maximum rotational speed of the fence drive system $\dot{\alpha}_{w_{max}} = 1.53\,\mathrm{rad/s}$, fence of length $R_z = 1.2\,\mathrm{m}$, time of fence working cycle $t_c = 1.36\,\mathrm{s}$), the deflection of fence tip did not exceed approx. $0.08\,\mathrm{m}$ (Fig. 8b, Fig. 9b, Fig. 10b).

The results of simulation shown in Fig. 8, pertaining to two variants of the fences (partly flexible, and fully flexible one), are almost identical. The lines in graphs in Fig. 8a and 8d representing the mentioned fence variants (thin lines referring to one-link fence, and thick lines for two-link one) coincide along all their lengths.

The point where the object loses its contact with the fence lies out of the main conveyor area (Fig. 8a), which guarantees that the load is carried to a new direction of transport. The oscillatory motion of the fence fades down before the fence returns to its initial position (Fig. 8b), owing to which the following working cycles are free of disturbances that might result from the transients of previous cycles.

The courses of dynamic reactions, presented in Fig. 8c, which appear during the impact between the object and the fence with flexible link (N), and between this object and an undeformable obstacle of infinite mass (N_{stiff}) are expressed in terms of relative values of the impact force N and N_{stiff}, referred

to the maximum impact force between the object and the fence with flexible link, N_{max}. It follows from the analysis of the obtained results that during the impact of the object against the flexible fence one can expect almost threefold decrease of dynamic reactions compared to those appearing when the object impacts against an undeformable, immobile obstacle (the one which represents a completely rigid fence joined with a rigid drive system; such a fence exerts most destructive effect on the manipulated loads).

In the course of impact, the friction force F_1 has, for most of the time, form of kinetic friction – Fig. 8d. The stage of static friction lasts a very short time – only approx. 0.003 s. For this reason, the chart of the friction force F_1 (in the initial course) makes up almost a vertical line.

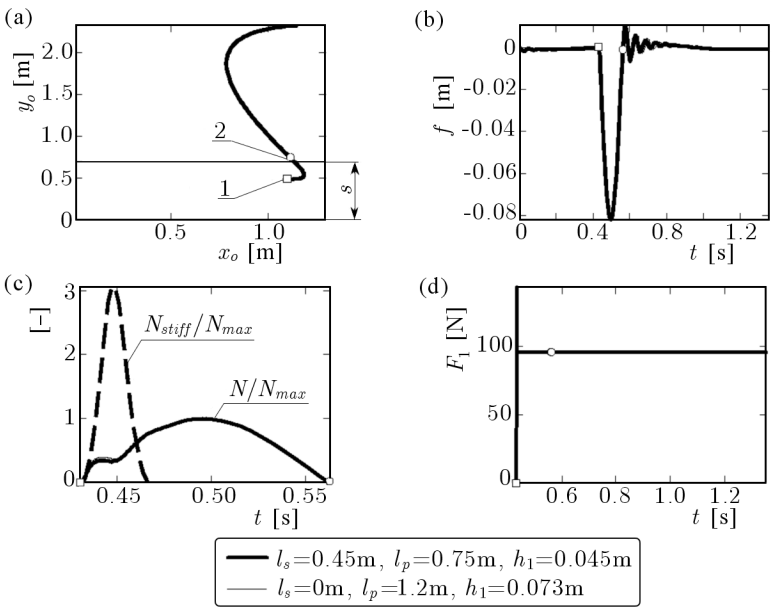

Fig. 8. Simulation results of object-against-fence impact (1 and 2 – beginning and end of impact, respectively): (a) motion trajectory of object gravity centre, (b) deflection of fence tip, (c) course of dynamic reactions during impact of load against fence (N), and against undeformable obstacle of infinite mass (N_{stiff}), (d) friction force F_1; process parameters: $b_p = 3.3 \cdot 10^5\,\mathrm{Nskg^{-0.4}m^{-3}}$, $k_p = 1.72 \cdot 10^9\,\mathrm{Nm^{-4}}$ (Piątkowski and Sempruch, 2009), $v = 2\,\mathrm{m/s}$, $m_p = 15\,\mathrm{kg}$, $\mu_{1k} = 0.65$, $\mu_{1s} = 0.85$, $\mu_{2k} = 0.35$, $\mu_{2s} = 0.5$, $n_E = 20$, $s = 0.7\,\mathrm{m}$

The effectiveness of softening the effects of impact of the load against the fence is illustrated in Fig. 9. Figure 9a pertains to the investigations results obtained for the fence consisting of two links ($l_s = 0.45\,\mathrm{m}$, $l_p = 0.75\,\mathrm{m}$), while Fig. 9b presents similar results for the one-link fence ($l_s = 0\,\mathrm{m}$, $l_p = 1.2\,\mathrm{m}$).

The effectiveness is expressed by a quotient of the force arising when the object impacts against an undeformable obstacle of infinite mass ($N_{stiff_{max}}$) to the force of impact for the flexible fence (N_{max}). The graphs are drawn in function of mass of the manipulated object m_p and the distance R between the contact point and the fence rotation axis ($R = 0$ pertains to the point where the fence is fixed, $R = 1.2\,\mathrm{m}$ – to its free end). The greater the mass of the object and the distance between the contact point and the fence axis, the greater the effectiveness of softening of the dynamic reactions arising in the impact (as one could predict).

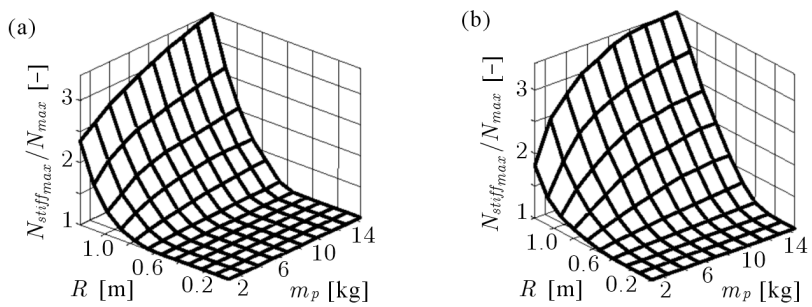

Fig. 9. Quotient of dynamic reaction forces exerted on object in impact against undeformable obstacle of infinite mass to reaction forces in impact against flexible link of fence: (a) fence consisting of rigid link and flexible link, (b) entirely flexible fence

The differences between the results obtained in investigation of the rigid-flexible fence, and those for the entirely rigid one, are insignificant. The drop of effectiveness of impact energy dissipation is only observed in the case when the point of contact between the load and the fence comes close to the joint between the rigid link and the flexible one. However, such a loss of the impact-softening effectiveness is not dangerous (as far as safety of the manipulated loads is concerned) – the greatest danger is associated with the impact of the object against the free end of the fence.

Similar relations also refer to the obtained deflection of the fence – Fig. 10. The increase of load mass m_p and distance R results in an increase of deflection of the fence tip. The discrepancies caused by structural differences between the examined fences are, also in this case, visible only in the vicinity of the joint between the rigid link and the flexible one (in the two-link fence).

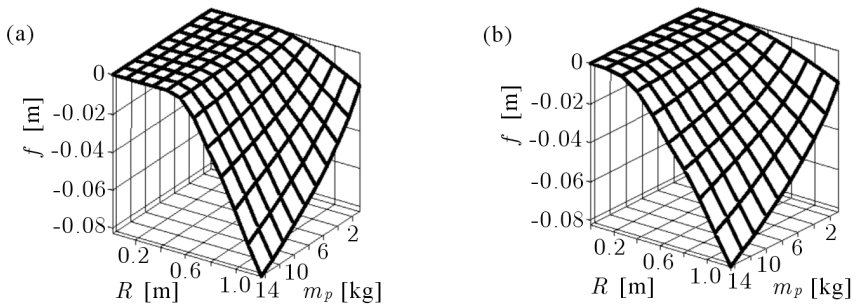

Fig. 10. Deflection of free end of fence: (a) fence consisting of rigid link and flexible link, (b) entirely flexible fence

3.2. Simulation of object motion along fence

The course of sorting process for the object which, before scrapping, lies near the border of the conveyor ($\Delta s = 0$) is shown in Fig. 11. In the investigations, we examined two variants of fences, whose structural parameters were consistent with the parameters used when deriving the data for Fig. 8-Fig. 10. Reference mark 1 indicates the moment of initiation of contact between the object and the fence, and reference mark 2 – the end of this contact.

The discrepancies between the test results obtained for the fence consisting of two links (rigid one, and flexible one) and those for the fence consisting of one (flexible) link are insignificant – similarly as it was in the cases presented in Fig. 8-Fig. 10. The two graphs, the one drawn in thick line (pertaining to the fence consisting of a rigid link and a flexible one), and the one drawn in thin line (pertaining to the entirely flexible fence) do not overlap only in Fig. 11b illustrating the course of deflection of the fence tip, and in Fig. 11c depicting the course of dynamic interactions between the object and the fence. A complete coincidence of these two graphs can be seen in Fig. 11a (representing trajectory of the object motion), and in Fig. 11d (where the course of the friction force F_1 is presented).

4. Conclusions

In this study, the author presented a proposal for the modelling of the process of sorting of unit load streams transported on belt conveyors by means of an active fence consisting of two links: a rigid and a flexible one. In the description of dynamic properties of the fence flexible link, the finite element method was

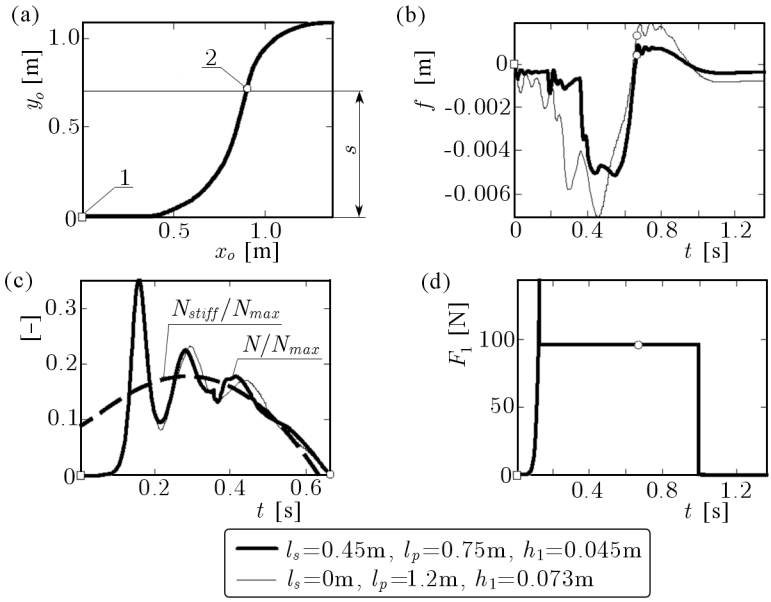

Fig. 11. Results of simulation of object motion along fence (1 – initiation of contact between object and fence, 2 – beginning of free motion of object): (a) motion trajectory of gravity centre of object, (b) deflection of fence tip, (c) courses of dynamic interactions between object and fence (N), and between object and undeformable obstacle of infinite mass (N_{stiff}), (d) friction force F_1; process parameters as in Fig. 8; N_{max} – maximum force of impact of object against flexible fence

applied. The reaction forces arising between the manipulated object and the fence were described with the use of a nonlinear Kelvin's model.

The developed model of the sorting process makes it possible to examine the influence of structural and operational parameters of the fence on the magnitude of forces exerted on the manipulated objects and on the course of motion of the object and the fence.

It follows from the performed simulation tests that by application of a rigid-flexible fence (consisting of two links, a rigid and a flexible one, with the length of the rigid link even as large as 1/3 of the fence total length), one can obtain similar effects of reducing the dynamic overloads exerted on the manipulated objects and a similar course of the distribution process as in the case when an entirely-flexible fence is applied.

This work has been financed from the funds for science as a Research Project in the years 2008-2010.

References

1. Akella S., Huang W.H., Lynch K.M., Mason M.T., 2000, Parts feeding on a conveyor with a one joint robot, *Algorithmica*, **26**, 313-344
2. Akella S., Mason M.T.,1998, Posing polygonal objects in the plane by pushing, *The International Journal of Robotics Research*, **17**, 70-88
3. Basf technical resources, accessed 2008-11-07, www.campusplastics.com
4. Berretty R.P., Goldberg K.Y., Overmars M.H., Stappen A.F., 1998, Computing fence designs for orienting parts, *Computational Geometry*, **10**, 249-262
5. Gawroński W., Kruszewski J., Ostachowicz W., Tarnowski J., Wittbrodt E., 1984, *Finite element method in construction dynamics*, Arkady, Warsaw
6. Giergiel J., 1990, *Tłumienie drgań mechanicznych*, PWN, Warszawa
7. Goyal S., Ruina A., Papadopoulos J., 1991, Planar sliding with dry friction. Part 1. Limit surface and moment function, *Wear*, **143**, 307-330
8. Jalili N., Esmailzadeh E., 2002, Dynamic interaction of vehicles moving on uniform bridges, *Journal of Multi-body Dynamics*, **216**, 343-350
9. Kikuuwe R., Takesue N., Sano A., Mochiyama H., Fujimoto H., 2005, Fixed-step friction simulation: from classical Coulomb model to modern continuous models, *Proceedings of IEEE/RSJ International Conference on Intelligent Robots and Systems*, Edmonton, Canada, 3910-3917
10. Mason M.T., 1986, Mechanics and planning of manipulator pushing operations, *The International Journal of Robotics Research*, **5**, 53-71
11. Mason M.T., 1999, Progress in nonprehensile manipulation, *The International Journal of Robotics Research*, **18**, 1129-1141
12. Piątkowski T., 2004, Active fence with pneumatic drive, *Pneumatyka*, **47**, 4, 24-27
13. Piątkowski T., Sempruch J., 2002, Sorting process of load units – dynamic model of scraping process, *The Archive of Mechanical Engineering*, **49**, 23-46
14. Piątkowski T., Sempruch J., 2005, Modelling of curvilinear scraper arm geometry, *The Archive of Mechanical Engineering*, **52**, 221-245
15. Piątkowski T., Sempruch J., 2006, Active fence with flexible element in a drive system, *The Archive of Mechanical Engineering*, **53**, 335-354
16. Piątkowski T., Sempruch J., 2008, Model of the process of load unit stream sorting by means of flexible active fence, *Mechanism and Machine Theory*, **43**, 5, 549-564, DOI: 10.1016/j.mechmachtheory.2007.05.004

17. Piątkowski T., Sempruch J., 2009, Model of inelastic impact of unit loads, *Packaging Technology and Science*, **22**, 39-51, DOI: 10.1002/pts.825

18. Stappen A.F., Goldberg K., Overmars M.H., 2000, Geometric eccentricity and the complexity of manipulation plans, *Algorithmica*, **26**, 494-514

19. Wittbrodt E., Adamiec-Wójcik I., Wojciech S., 2006, *Dynamics of Flexible Multibody Systems – Rigid Finite Element Method*, Springer-Verlag, Berlin, Germany

20. Zienkiewicz O.C., 2000, *The Finite Element Method*, Butterworth-Heinemann, Oxford, UK

Zastawa aktywna z członem podatnym

Streszczenie

W artykule przedstawiono wyniki badań modelu procesu sortowania strumienia ładunków jednostkowych zastawą aktywną o jednym stopniu swobody. Podczas badań manipulowane ładunki traktowane są jako ciała o nieliniowych właściwościach sprężysto-tłumiących. W konstrukcji zastawy uwzględniono człon sztywny i połączony z nim człon podatny. Równania ruchu członu podatnego zastawy i wchodzącego z nim w interakcje obiektu wyprowadzono w oparciu o metodę elementów skończonych (MES). Odpowiednie kształtowanie parametrów konstrukcyjnych członu podatnego zastawy pozwala wpływać na złagodzenie oddziaływań dynamicznych wywieranych na sortowane ładunki.

Manuscript received March 2, 2009; accepted for print May 11, 2009